Biosensors and Bioelectronics 144 (2019) 111686

Contents lists available at ScienceDirect

Biosensors and Bioelectronics

journal homepage: www.elsevier.com/locate/bios

Paper-based 3D culture device integrated with electrochemical sensor for the on-line cell viability evaluation of amyloid-beta peptide induced damage in PC12 cells

Meng-Meng Liu[1], Zi-Zhen Guo[1], Hui Liu, Shan-Hong Li, Yao Chen, Yu Zhong, Yun Lei[**], Xin-Hua Lin[***], Ai-Lin Liu[*]

Department of Pharmaceutical Analysis, Higher Educational Key Laboratory for Nano Biomedical Technology of Fujian Province, Faculty of Pharmacy, Fujian Medical University, Fuzhou, 350122, China

ARTICLE INFO

Keywords:
Paper-based 3D cell culture device
On-line cell viability evaluation
Dopamine
PC12 cells
Amyloid-beta peptide

ABSTRACT

In this communication, a paper-based 3D cell culture device integrated with electrochemical biosensor was applied to on-line monitoring of dopamine release from PC12 cell damage models induced by amyloid-beta peptide ($A\beta_{25\text{-}35}$) and cell intervene models protected by curcumin (Cur) and marrow mesenchymal stem cells (MSC) supernatant. The adhesion and proliferation of PC12 cells cultured on the paper scaffold was characterized by scanning electron microscopy and laser scanning confocal microscopy, which verify unique biocompatibility and 3D microarchitecture similar to human body microenvironment of paper substrate, so an artificial model simulating 3D microenvironment *in vivo* was constructed easily. The PC12 cells in paper-based devices consisted of four groups containing control group, $A\beta_{25\text{-}35}$ group, $A\beta_{25\text{-}35}$ + Cur group and $A\beta_{25\text{-}35}$ + MSC supernatant group. Under optimal conditions, this proposed device displayed a wide linear range from 0.05 to 1 μmol/L with a detection limit of 0.009 μmol/L (S/N = 3) and exhibited high sensitivity, good selectivity and excellent reproducibility. Furtherly, electrochemcial analysis and MTT assay gave a clue that the cell viability of $A\beta_{25\text{-}35}$ + MSCs supernatant group was higher than that of $A\beta_{25\text{-}35}$ + Cur group. Therefore, the detachable paper-based 3D device paves the way to a direct detection of exocytosis DA from neuron cells for on-line cell viability evaluation of neurodegenerative disease cell damage models.

1. Introduction

Cell damage models played an important role in researching the causes and seeking the effective treatments for diagnosing and treating patients with the neurodegenerative disease, such as Alzheimer's disease, Parkinson's disease, Huntington's disease and many others (Iannielli et al., 2018; Ross et al., 2018; Siebzehnrübl et al., 2018). Current methods for construction of cell damage models are relying on physical and chemical manner, for instance, radiation and small organic molecules induction, and so on. The features of cell damage models are that they could stimulate certain pathological characteristics of a disorder, providing relevant information of the physiological and pathological process, mechanisms of drugs effect and drugs screening related to neurodegenerative diseases. Taking alzheimer's disease as an example, neurogenic cells (e.g. PC12, SH-SY5Y, NG108-15 and SK-N-SH cells) are usually used as research objectives to construct cell damage model induced by amyloid-beta peptide, hydrogen peroxide and okadaic acid for studying the mechanisms of apoptosis and drug actions (Benseny-Cases et al., 2018; Forest et al., 2018; Pascual-Caro et al., 2018; Velagapudi et al., 2016).

Moreover, cell damage models constructed on traditional two-dimensional (2D) culture interface could not effectively reflect the critical structural and biochemical information providing misleading and false positive results for *in vivo* due to the original property change of cell morphology and heterogeneity. In contrast, the three-dimensional (3D) cell culture platform can improve cell viability, adhesion, proliferation and migration and mimic a 3D microenvironment to replicate the real physiological scenario to a degree for the drug screening outcomes, and

* Corresponding author.
** Corresponding author.
*** Corresponding author.
E-mail addresses: lypiglet@163.com (Y. Lei), xhl1963@sina.com (X.-H. Lin), ailinliu@fjmu.edu.cn (A.-L. Liu).
[1] Meng-Meng Liu and Zi-Zhen Guo contributed equally to this work.

https://doi.org/10.1016/j.bios.2019.111686
Received 7 August 2019; Received in revised form 4 September 2019; Accepted 5 September 2019
Available online 05 September 2019
0956-5663/

have drawn great researchers' attention (Ekerdt et al., 2018; Huh et al., 2011; Kraniak et al., 2018; Lou et al., 2018). However, 3D culture platform is difficult for conventional optical microscope to observe cell viability in real time. Hence, monitoring peculiar neurotransmitter molecules secreted by cell damage models of neurodegenerative diseases with the simple 3D culture platform has gathered more and more scientific focus to develop real-time monitoring cell viability systems.

The electrochemical sensor, for its remarkable advantages of fast response, excellent selectivity, high sensitivity, low-cost detection, real-time monitoring and being easy to develop point-of-care test, has been successfully applied in abundant fields ranging from analytical chemistry to biochemistry, environment and medicine (Gebicki, 2016; Maduraiveeran et al., 2018; Wang et al., 2018). Recently, many researchers devoted themselves to develop 3D scaffolds (e.g. 3D nanostructure layouts, 3D scaffold coating with conductive and biocompatibility polymer, 3D matrigel) for direct cell culture with the electrochemical sensors (Alegret et al., 2018; Hu et al., 2018; Lee et al., 2018). Paper, as an alternative for the 3D cell culture substrates, is a flexible, biocompatible and micro-nanofibrous material that has many advantages compared to traditional 3D scaffolds. The unique features of paper are introduced as follows: (1) readily available and low cost; (2) highly porous and good biocompatible; (3) can be flexible cut, folded, rolled and stacked; (4) easy to sterilization, physicochemical modification; (5) easy to construct normal and disease models; (6) micro-nanofibrous structure can replicate a 3D microenvironment (Bai et al., 2018; Li et al., 2019; Michael et al., 2018; Pupinyo et al., 2019; Whitman et al., 2018). Kenney's group combined paper substrate and pH-sensing optodes together for mapping spatial and temporal pH gradients of cells in 3D culture systems (Kenney et al., 2018).

In this communication, our group constructs an integrated paper-based 3D cell culture device combining with the screen-printed carbon electrode (SPCE) modified with gold nanoparticles (Au NPs) and nafion for 3D cell culture and on-line cell viability evalution by on-line detection of exocytosis dopamine (DA) in cell damage models. Specifically, as illustrated in Scheme 1, PC12 cell damage models of Alzheimer's disease-like pathological changes induced by amyloid-beta peptide ($A\beta_{25\text{-}35}$) was used as an experimental model of neurodegenerater diseases. The proposed paper-based device was used to mimic a 3D cell culture microenvironment. Then cell intervention models protected by curcumin (Cur) and bone marrow mesenchymal stem cell line supernatant (MSCs), named as $A\beta_{25\text{-}35}$ + Cur group and $A\beta_{25\text{-}35}$ + MSCs supernatant group, was constructed in paper-based 3D devices. In order to evaluate cell viability, the electrochemical sensor was applied to detect released DA from living cells of the four model groups including the control group, the $A\beta_{25\text{-}35}$ group, the $A\beta_{25\text{-}35}$ + Cur group and the $A\beta_{25\text{-}35}$ + MSCs supernatant group by differential pulse voltammetry. At the same time, MTT assay was performed accordingly with the four model groups. The level of exocytosis DA is consistent with the cell viability of MTT from the four group, implying that the combination of paper-based 3D device provides a universal platform for the evaluation of cell viability.

2. Experimental section

Materials, apparatus, fabrication and characterization of the paper-based 3D culture device can be referred in Supplementary information.

3. Results and discussion

3.1. Proliferation and characterization of cells in the paper-based 3D culture device

To verify the proliferation ability of cells on the paper-based 3D culture device, PC12 cells were seeded in the paper and cultured for several days. Cells imaging was successfully performed using GFP labelled PC12 cells on the day of 1, 2 and 3 after culturing (Fig. 1). As shown in Fig. 1a, PC12 cells were distributed uniformly on the filter paper by capillary wicking of fibers and only a small number of cells were observed on the day 1 after culturing. The clones of PC12 cells gradually become larger and fluorescence intensity progressively enhanced with the culture time lasting (shown in Fig. 1b and c). The fastest cell growth was appeared after 2 days of culture, leading to a dense cell population in the surface of paper and gaps between fibers (Fig. 1c). The results demonstrate the paper-based 3D culture device could furnish a biocompatible environment for cell culture without affecting the proliferation ability of PC12 cells.

The adhesion and cell morphology are further characterized by laser scanning confocal microscopy and scanning electron microscopy (SEM), which is different from those spread on the surface of tissue culture polystyrene. From fluorescent images, confocal z-stacked images of cells attached to paper fiber displayed the uniform distribution of cells on various heights (Fig. 1d and f). Fig. 1e was the 3D reconstruction of filter paper with 100 μm thick. The cells randomly distribute in different areas and heights of paper by capillary wicking (Fig. 1f). From SEM images, the filter paper fibers did not provide a flat surface for cell adhesion (Fig. 1g and h). Some cells formed clusters in 3D microenvironment surrounded by filter fibers on filter paper while others distributed singly (Fig. 1g). Spheroid-like structure of PC12 cells randomly distributed on the surface of fiber or the gap between fibers which was in accordance with the confocal images.

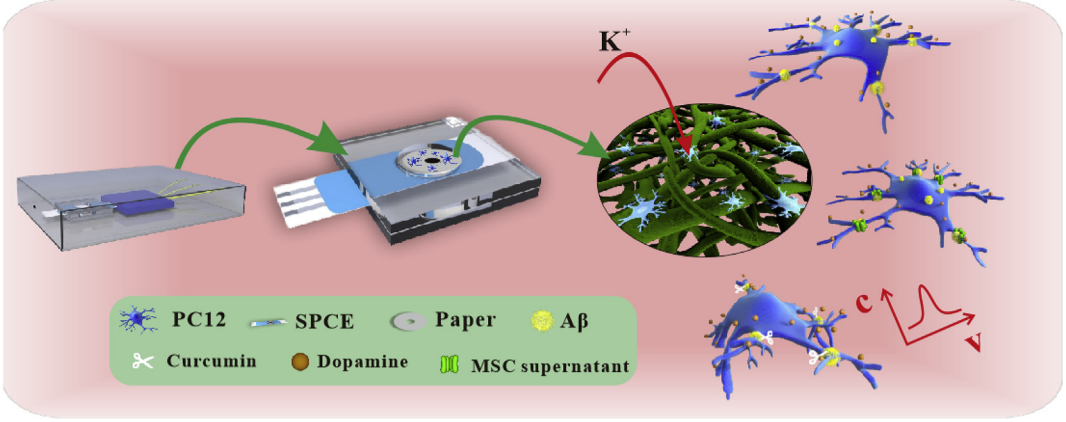

Scheme 1. Schematic representation of the paper-based 3D culture devices for detection of released dopamine by PC12 cells.

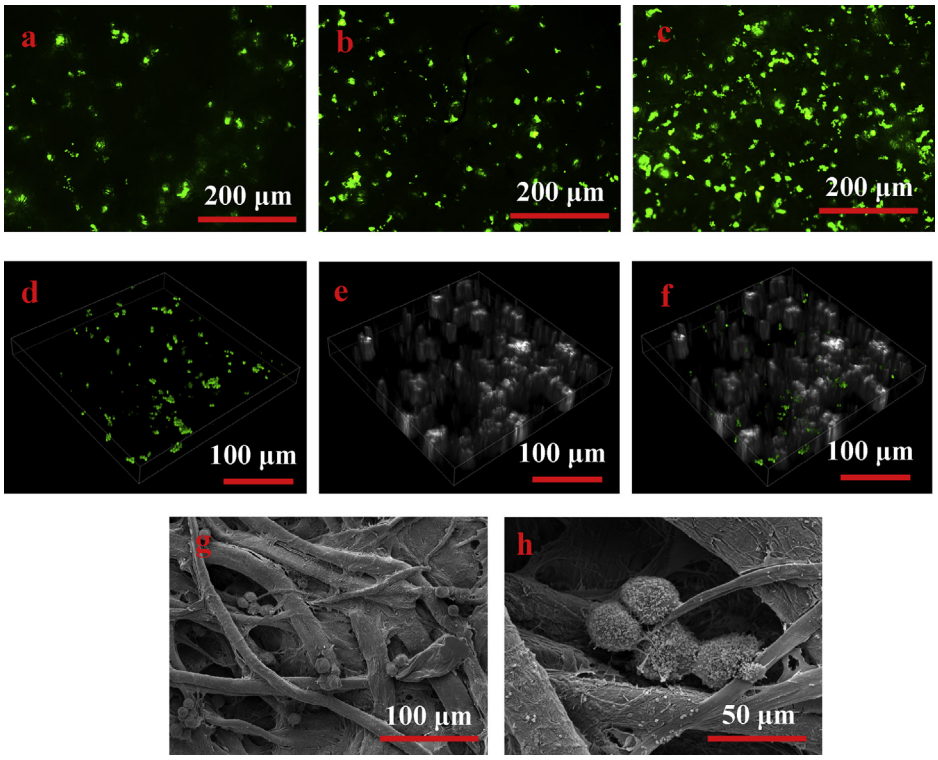

Fig. 1. Fluorescent images of PC12 cells cultured on filter paper for 24 h (a), 48 h (b) and 72 h (c). Laser scanning confocal microscopy images of 3D reconstruction for PC12 cells (d) cultured on filter paper (e) and merged images of PC12 cells and paper fibers (f). SEM images of PC12 cells cultured on paper scaffold with low resolution (g) and high resolution (h).

3.2. Performance of electrochemical sensor in the paper-based 3D culture device

3.2.1. Characterization of the electrochemical sensor in the paper-based 3D culture device

Field emission scanning electron microscope was selected to characterize the surface morphology of the SPCE before and after modification. The bare electrode is composed of micro-nano-sized, granular carbon powder, illustrating a porous and loosen structure at nano level resolution (shown in Fig. S2). The flower-like, scattered electrodeposited Au NPs on the SPCE possesses high specific surface area which is favor of signal amplification (shown in Fig. 2A). Chemical composition analysis of the modified SPCE was obtained by energy dispersive spectrometer (EDS), providing direct evidence for the existence for C and Au elements (shown in Fig. 2B). The properties of nafion/Au NPs/SPCE were evaluated by cyclic voltammetric in H_2SO_4 solution (shown in Fig. S3). There is no redox peak of Au in the bare SPCE (curve a), while Au NPs/SPCE and nafion/Au NPs/SPCE have characteristic reductive peak of gold at the potential of 0.5 V and oxidation peak of gold at the potential of 1.0 V (curve b and c). The eminent stability of nafion film is beneficial to construct a charge sensor to protect the electrode's surface from superfluous adsorption and poisoning and enhance selectivity via electrostatic repulsion.

3.2.2. Detection of DA

Under the optimum conditions, the calibration plot was obtained by detecting DA prepared with PBS. As shown in Fig. 2C, the current of oxidation peak measured by DPV increases gradually with increasing DA concentrations. The peak current of DA enhances linearly with the concentration of DA range from 0.05 to 100 μmol/L (Fig. 2C, insert). The regression equation is $I(\mu A) = 0.3410 + 0.0071\ C_{DA}$ (μmol/L) with the correlation coefficient of 0.9977. The limit of detection (LOD) at 3σ is 0.0059 μmol/L. To confirm the potential applicability of this sensor in more complex bio-samples such as cells, a series of various concentrations of DA were prepared by PBS-incubated with PC12 cells. Typical DPV responses to the increase of DA with corresponding linear regression illustrated in Fig. 2D. The linear regression is described as follows: $I(\mu A) = 0.01679 + 0.2718\ C_{DA}$ (μmol/L), $R^2 = 0.9949$ (Fig. 2D, insert), with the detection limit of 0.009 μmol/L (S/N = 3). The results indicate that this proposed sensor could be used to detect DA in complex bio-samples with satisfactory accuracy.

3.3. PC12 cells viability evaluation by monitoring released DA from cell damage models

The release of DA from PC12 cells was seriously impacted by cell viability and induced final state (Barlow et al., 2018). To assess the cell activity of the cell models, the cells cultured in the paper chip are divided into four model groups including control group, $A\beta_{25\text{-}35}$ group, $A\beta_{25\text{-}35}$ + Cur group and $A\beta_{25\text{-}35}$ + MSCs supernatant group (shown in Fig. 2E, Scheme of cell activity evaluation). As shown in Fig. 2E, DPV response of released DA from each group was recorded after stimulating PC12 cells with 105 mmol/L K^+ solution. From Fig. S12, the peak current of released DA was obtained in $A\beta_{25\text{-}35}$ group indicating PC12 cells suffer severe cytotoxic of $A\beta_{25\text{-}35}$ while the peak current of released DA from $A\beta_{25\text{-}35}$ + Cur group and $A\beta_{25\text{-}35}$ + MSCs supernatant group intensified on various degrees owing to neuroprotective effects of curcumin and MSCs supernatant. Compared to control group, the release of DA from the $A\beta_{25\text{-}35}$ group down regulates to 37% while the release of DA falls to 52.57% and 85.27% from $A\beta_{25\text{-}35}$ + Cur group and $A\beta_{25\text{-}35}$ + MSCs supernatant group, respectively (shown in Fig. 2F). MTT assay showed that PC12 cells pre-treated with curcumin and MSCs supernatant for 6 h markedly up-regulated the cell viability from 44% to 63.36% and 73.56%, respectively (shown in Fig. 2F). The results indicated that cell viability is basically consistent with DA secretion capacity of cells. And the intervention effect of MSCs supernatant is stronger than curcumin, supplying new direction for treatment of neurodegenerative disorders. However, there is a little difference related to numerical value of cell viability between MTT and this proposed 3D device which may be caused by different assessing factors. MTT assay is based on the ability of mitochondrial dehydrogenase in living cells to transform the water-soluble tetrazolium salt into formazan crystals. The production of MTT-formazan is proportional to the number of metabolically viable cells. While, the paper-based 3D cell

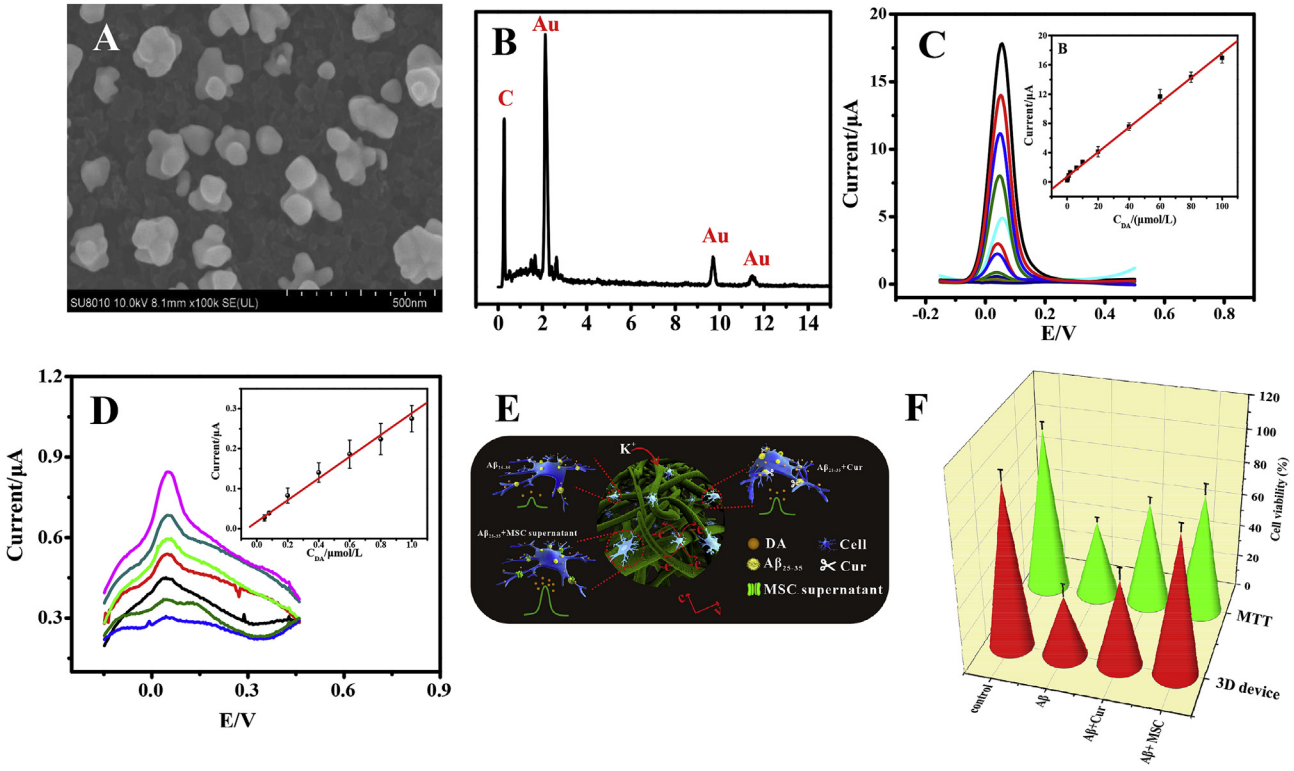

Fig. 2. (A) SEM images of screen-printed carbon electrode modified with Au NPs. (B) Energy dispersive spectrometer spectrum of Au NPs/SPCE. (C) DPV responses to different concentrations of DA prepared by PBS (0.1 mol/L, pH = 7.4). Inset of C: Linear relationship between current value and concentrations of DA. (D) DPV responses to different concentrations of dopamine prepared by PBS-incubated with PC12 cells (0.1 mol/L, pH = 7.4). Inset of D: Linear relationship between current and concentrations of DA. (E) Scheme showing drugs effect on PC12 cells cultured on paper-based 3D culture devices. (F) Comparison of cell activities between the paper-based 3D culture device and MTT.

culture device is evaluated by the release of neurotransmitters from living cells, tending to biological characteristics aspect.

4. Conclusions

In summary, the paper-based 3D culture device was fabricated for 3D cell culture and on-line monitoring of released dopamine from PC12 cell damage models. The porosity of cellulose paper is preferable for cell adhesion and proliferation, providing inherent 3D micro-architecture similar to human body microenvironment. The PC12 cells cultured on this device were treated with different drugs and divided into four groups to reflect changes of corresponding pathological process of cell models. The results of the developed device demonstrated the repair action of MSCs supernatant is stronger than that of curcumin. Further application of this device may offer a promising 3D cell culture and on-line cell viability evaluation for drug screening, facilitating studies of physiological and pathological relevant processes.

CRediT authorship contribution statement

Meng-Meng Liu: Investigation, Writing - original draft. **Zi-Zhen Guo:** Investigation, Writing - original draft. **Hui Liu:** Investigation. **Shan-Hong Li:** Investigation. **Yao Chen:** Investigation. **Yu Zhong:** Investigation. **Yun Lei:** Project administration, Writing - review & editing. **Xin-Hua Lin:** Project administration, Supervision. **Ai-Lin Liu:** Conceptualization, Funding acquisition, Methodology, Project administration, Writing - review & editing.

Declaration of competing interest

The authors declare that they have no known competing financial interests or personal relationships that could have appeared to influence the work reported in this paper.

Acknowledgments

The authors gratefully acknowledge the financial support of the National Natural Science Foundation of China (21775023), the Natural Science Foundation of Fujian Province of China (2014J07009), Joint Funds for the Innovation of Science and Technology, Fujian Province (2016Y9055), and Social Development Guiding Programs of Fujian Province of China (2019Y0012).

Appendix A. Supplementary data

Supplementary data to this article can be found online at https://doi.org/10.1016/j.bios.2019.111686.

References

Alegret, N., Dominguez-Alfaro, A., Mecerreyes, D., 2018. Biomacromolecules 20, 73–89.
Bai, R.H., Li, L.M., Liu, M.M., Yan, S.Q., Miao, C.Y., Li, R.J., Luo, Y., Liu, T.J., Lin, B.C., Ji, Y.B., Lu, Y., 2018. Anal. Chem. 90, 5825–5832.
Barlow, S.T., Louie, M., Hao, R., Defnet, P.A., Zhang, B., 2018. Anal. Chem. 90, 10049–10055.
Benseny Cases, N.R., Álvarez-Marimon, E., Castillo-Michel, H., Cotte, M., Falcon, C., Cladera, J., 2018. Anal. Chem. 90, 2772–2779.
Ekerdt, B.L., Fuentes, C.M., Lei, Y., Adil, M.M., Ramasubramanian, A., Segalman, R.A., Schaffer, D.V., 2018. Adv. Healthc. Mater. 7, 1800225.
Forest, K.H., Alfulaij, N., Arora, K., Taketa, R., Sherrin, T., Todorovic, C., Lawrence, J.L., Yoshikawa, G.T., Ng, H.L., Hruby, V.J., 2018. J. Neurochem. 144, 201–217.
Gebicki, J., 2016. Trac. Trends Anal. Chem. 77, 1–13.
Hu, X.B., Liu, Y.L., Wang, W.J., Zhang, H.W., Qin, Y., Guo, S., Zhang, X.W., Fu, L., Huang, W.H., 2018. Anal. Chem. 90, 1136–1141.
Huh, D., Hamilton, G.A., Ingber, D.E., 2011. Trends Cell Biol. 21, 745–754.
Iannielli, A., Bido, S., Folladori, L., Segnali, A., Cancellieri, C., Maresca, A., Massimino, L., Rubio, A., Morabito, G., Caporali, L., 2018. Cell Rep. 22, 2066–2079.
Kenney, R.M., Boyce, M.W., Whitman, N.A., Kromhout, B.P., Lockett, M.R., 2018. Anal.

Chem. 90, 2376–2383.
Kraniak, J.M., Chalasani, A., Wallace, M.R., Mattingly, R.R., 2018. Exp. Neurol. 299, 289–298.
Lee, S.J., Zhu, W., Nowicki, M., Lee, G., Heo, D.N., Kim, J., Zuo, Y.Y., Zhang, L.J.G., 2018. J. Neural Eng. 15, 016018.
Li, J., Liu, X., Tomaskovic-Crook, E., Crook, J.M., 2019. Colloids Surf., B 176, 87–95.
Lou, J.Z., Stowers, R., Nam, S.M., Xia, Y., Chaudhuri, O., 2018. Biomaterials 154, 213–222.
Maduraiveeran, G., Sasidharan, M., Ganesan, V., 2018. Biosens. Bioelectron. 103, 113–129.
Michael, I.J., Kumar, S., Oh, J.M., Kim, D.Y., Kim, J.Y., Cho, Y.K., 2018. ACS Appl. Mater. Interfaces 10, 33839–33846.
Pascual-Caro, C., Berrocal, M., Lopez-Guerrero, A.M., Alvarez-Barrientos, A., Pozo-Guisado, E., Gutierrez-Merino, C., Mata, A.M., Martin-Romero, F.J., 2018. J. Mol. Med. 96, 1061–1079.
Pupinyo, N., Chatatikun, M., Chiabchalard, A., Laiwattanapaisal, W., 2019. Analyst 144, 290–298.
Ross, S.P., Baker, K.E., Fisher, A., Hoff, L., Pak, E.S., Murashov, A.K., 2018. Front. Cell. Neurosci. 12, 87–96.
Siebzehnrübl, F.A., Raber, K.A., Urbach, Y.K., Schulze-Krebs, A., Canneva, F., Moceri, S., Habermeyer, J., Achoui, D., Gupta, B., Steindler, D.A., 2018. Proc. Natl. Acad. Sci. U.S.A. 115, 8765–8774.
Velagapudi, R., Baco, G., Khela, S., Okorji, U., Olajide, O., 2016. Eur. J. Nutr. 55, 1653–1660.
Wang, Y.W., Liu, Y.L., Xu, J.Q., Qin, Y., Huang, W.H., 2018. Anal. Chem. 90, 5977–5981.
Whitman, N.A., Lin, Z.W., DiProspero, T.J., McIntosh, J.C., Lockett, M.R., 2018. Anal. Chem. 90, 11981–11988.